Experimental Investigation on the Bond Behavior of Steel Fiber Reinforced Mortar (SFRM) applied onto Masonry Substrates

Nicolò SIMONCELLO [1], Jaime GONZALEZ-LIBREROS [1], Paolo ZAMPIERI [1], Carlo PELLEGRINO [1]

[1] University of Padua, Padua, Italy

Contact e-mail: jaime.gonzalez@dicea.unipd.it

ABSTRACT: Due to its low tensile strength and brittle behavior, the use of concrete as structural material has required the use of tensile reinforcement, traditionally on the form of reinforcing bars placed on the locations in which high tensile stresses are expected. In previous decades, the use of steel, glass, or plastic fibers dispersed randomly on the fresh concrete mix for the total or partial replacement of reinforcing bars has shown to provide significant increase on the tensile and flexural strength, abrasion resistance, permeability, toughness and durability of concrete. The use of this composite material, known as fiber reinforced concrete (FRC) or mortar (FRM), for industrial pavement, tunnel linings, and hydraulic and precast structures has shown satisfactory results. More recently, the use of FRC and FRM for the strengthening of existing concrete and masonry structures has caught the attention of researchers worldwide. Unfortunately, experimental evidence on the topic is still scarce and a significant research effort is required to gain knowledge about the behavior of structures strengthened using these materials. Based on this need, in this paper the bond behavior of steel fiber reinforced mortar (SFRM) applied onto masonry supports is investigated by means of double-lap shear tests. Results of the tests are discussed in terms of load response, and failure mode.

1   INTRODUCTION

The need of repairing and retrofitting of existing masonry structures has led to the continuous search and development of cost/efficient techniques that guarantee an appropriate behavior of the structure after the strengthening. Among the techniques available now, the use of fiber reinforced polymer (FRP) composites has gained worldwide popularity due to their ability to increase the structure strength, combined with advantages such a high strength to weight ratio, and ease and speed of application, among others (Tetta and Bournas, 2016). However, drawbacks of the FRP composites, mainly related to the resins, such as poor behavior at high temperatures, lack of vapor permeability, and incompatibility of the epoxy resins with the substrate materials have been recently pointed out (Triantafillou and Papanicolaou, 2006). More recently, the use of fiber reinforced cementitious matrix (FRCM) composites for the strengthening of existing structures, have shown promising results (De Stefano, *et al.*, 2017; Gonzalez-Libreros, *et al.*, 2017; Carozzi, *et al.*, 2018).   Replacing the organic resins by an inorganic one allows overcoming some of the drawbacks associated to the use of FRP composites. However, available experimental evidence has shown that FRCM composites might provide a reduced increase in the strength, when compared to their FRP counterparts (Tetta, Koutas and Bournas, 2015; Gonzalez-Libreros, *et al.*, 2017).

Recently, the use of fiber reinforced mortars (FRM), comprised of high strength mortars and short fibers, for the strengthening of existing structures have caught the attention of researchers

(Sevil, *et al.*, 2011; Tsonos, 2014). The addition of fibers in the mortar has proven to increase on the tensile and flexural strength, abrasion resistance, permeability, toughness and durability of the material (Altun, Haktanir and Ari, 2007). Under tensile loading, SFRM exhibits fine and well distributed cracking accompanied by large inelastic deformation prior to reaching failure which makes them suitable for repair and strengthening (Müller and Mechtcherine, 2018). With the aim of improving the knowledge about this material and its use for strengthening of masonry structures, the bond behavior of steel FRM (SFRM) applied onto masonry substrates is investigated in this paper. The bonding behavior of composites has proven to be fundamental for the development of formulations to predict the increase of strength provided by the composites (ACI Committee 440, 2008; National Research Council (CNR), 2013). For the case of FRP and FRCM composites, the bond behavior has been investigated mainly using single-lap or double-lap direct shear tests (Sneed, *et al.*, 2015; Askouni and Papanicolaou, 2017; Ombres, *et al.*, 2019). In this paper, the double-shear lap configuration was chosen to evaluate the bond behavior of SFRM strips applied onto masonry structures. Results are discussed in terms of maximum applied load and failure mode.

2 EXPERIMENTAL CAMPAIGN

The experimental campaign presented in this paper focuses on the bond behavior of SFRM strips applied onto masonry substrate. With this end, three specimens comprised of two masonry prisms connected through a SFRM strip on each sided were built and tested using a double-lap direct-shear configuration.

2.1 Materials

The masonry prisms used in this research were made with standard clay bricks with nominal dimensions equal to 245x110x60 mm and mortar bed joints with a thickness of 10 mm. Values of compressive strength, and elastic modulus of the bricks, as reported by the producer, are presented in Table 1. In order to replicate the actual condition of existing structures, a low cementitious mortar was used for the specimen's joints (Type M5). Average values of the main mechanical properties of the mortar, experimentally evaluated in the laboratory according to UNI 1015-11, 2007 and UNI EN 13412, 2006, are included in Table 1.

Table 1. Mechanical properties of the materials

Material	Compressive strength [MPa]	Flexural strength [MPa]	Tensile strength [MPa]	Elastic Modulus [MPa]
Brick	18.8	-	-	9024
Mortar	7.22	2.22	-	3706
SFRM	91.02	15.43	4.5 (6.0)*	24040

* Tensile strength at first crack (maximum tensile strength at failure)

The SFRM is comprised of a high strength mortar fiber-reinforced with around 2% of hook end steel fibers in volume (see Figure 1). Experimental values of compressive and flexural strength, and elastic modulus for the SFRM material, evaluated according to the same standards used for the bed joint mortar, are included in Table 1. Table 1 also includes values of tensile strength at first crack and maximum tensile strength (in parenthesis in Table 1) reported by the SFRM provider.

Figure 1. SFRM Material.

2.2 Test set-up

Two SFRM strips were bonded to the surface of two masonry prisms (one on each side). The SFRM strips had a thickness (t) of 30 mm, width (b) of 80 mm, and bonded (L_b) and total length equal to 150 mm and 380 mm, respectively (see Figure 2). The thickness of the SFRM strips was set equal to 30 mm, based on the limitation provided by the steel fibers length (30 mm, see Figure 1). The free space between the two prisms (named c in this paper) was set equal to 80 mm. During testing, a tensile force (F) is applied through steel bars connected to a steel plate at one end. The rods were inserted using holes previously drilled in the center of the masonry prisms and were then clamped to the testing machine. Tests were performed under displacement control with a constant rate of 0.84 mm/s on a universal testing machine with a 600 kN capacity.
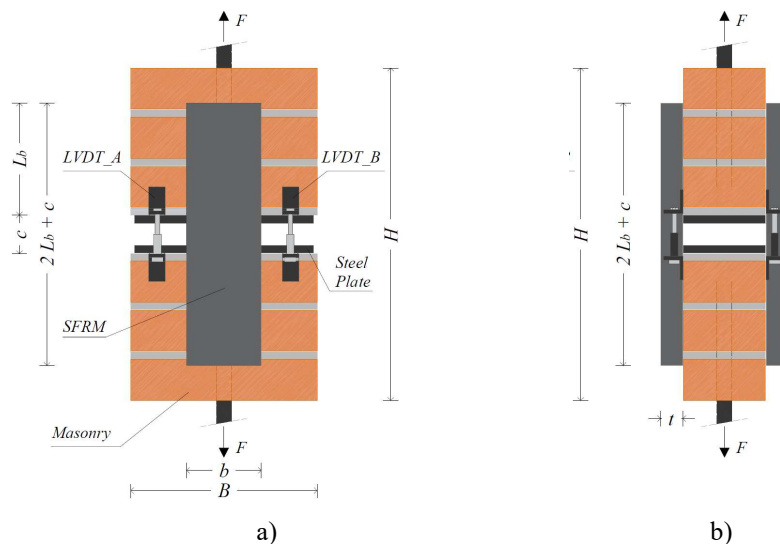

Figure 2. Test setup: a) Front view, b) side view

The displacement between the top and bottom masonry prisms was measured by means of four linear variable displacement transducer (LVDTs) applied on the masonry surface (two on each side, see Figure 2). Tests were named using the following convention: DSL_SFRM_XXX_#,

3

where DSL the type of test (double-shear lap test), XXX is the bonded length (L_b=150 mm for the three specimens), and # is the specimen number.

3 RESULTS AND DISCUSSION

3.1 Failure mode

Failure mode of the specimens was characterized by debonding of the SFRM strips from the substrate, cracking of the SFRM strips, or a combination of both. For specimen DSL_SFRM_150_001, as shown in Figure 3a, failure was attained by the development of cracks located at the middle of the unbonded area. Cracks started to be visible around peak applied force (F_{max}) and keep increasing their width with the increase in the displacement. Specimen DSL_SFRM_150_002 (see Figure 3b) failed due to early debonding of the SFRM strip from the masonry substrate at a value of F_{max} considerably lower than those attained for the other specimens (see section 3.2). For specimen DSL_SFRM_150_003, debonding of the SFRM strips from three out of the four bonded areas was witnessed (Figure 3c). However, before failure, transversal cracks in the unbonded region, as the ones observed for specimen DSL_SFRM_150_001, were also observed. As observed in Figures 3b and 3c, the debonding happened at the SFRM-masonry interface with a thin layer of masonry and bed joint mortar attached to the SFRM strip. This behavior is similar to that reported for FRP strips applied onto concrete or masonry substrates (Bellini and Mazzotti, 2017; Vaculik, *et al.*, 2018).
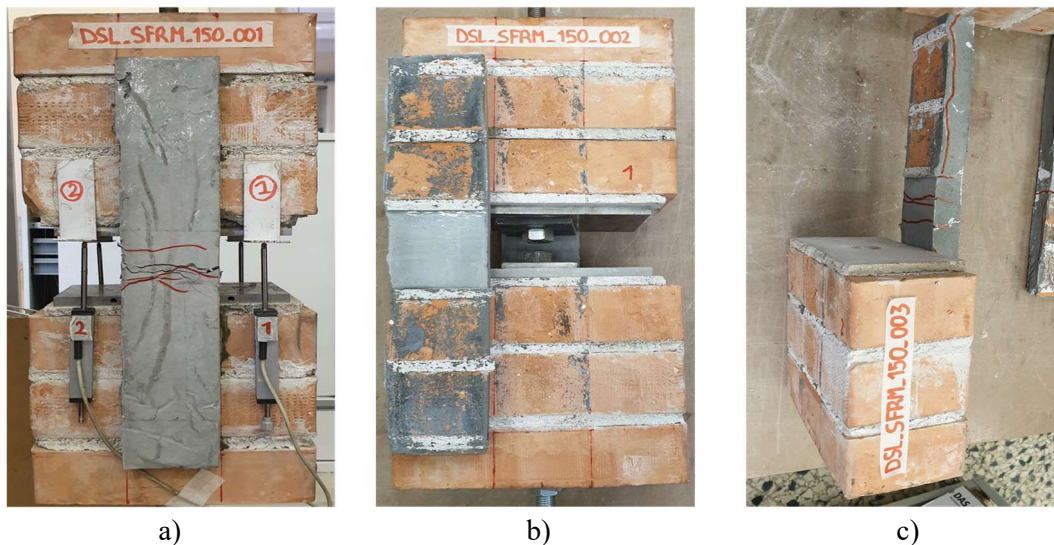

| a) | b) | c) |

Figure 3. Failure mode: a) DSL_SFRM_150_001, b) DSL_SFRM_150_002, c) DSL_SFRM_003

3.2 Applied load vs. displacement behavior

Figure 4 shows the applied load (P) versus displacement for the specimens studied. The value of P corresponds to force taken by each strip, assuming perfect symmetry, and is computed as shown in Eq. 1. The value of displacement shown in Figure 4 was computed as the average of the four LVDTs used during testing.
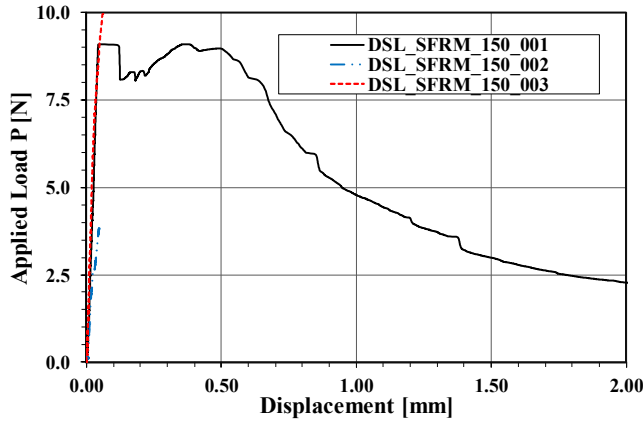
$$P = {}^{F}\!/_{2}$$ (1)

Figure 4. Applied load P vs. displacement

Figure 4 shows that the applied load P vs. displacement response is characterized by an initial linear ascending branch. It is interesting to note that, independently of the failure mode or maximum applied load (P_{max}), the slope of this branch is the same for the three specimens. For specimens DSL_SFRM_150_002 and DSL_SFRM_150_003, i.e., specimens that failed due to debonding, the applied load P vs. displacement response showed such linear behavior up to P_{max}. The response of specimen DSL_SFRM_150_001 shows a load drop, associated with the opening of the cracks in the unbonded region, immediately after P_{max} is attained. However, Figure 4 shows that the system can continue gaining strength after this point reaching a value of applied load similar to P_{max}. This behavior might be attributed to the presence of the steel fibers that bridge the cracks, allowing the increase in the applied load.

In Table 2, values of maximum applied force (F_{max}), applied load (P_{max}), stress in the SFRM strip in the unbonded region (σ_{max}), and SFRM-masonry bond shear stress (τ_{max}) for the three tested specimens are summarized. Table 2 includes also the average of these parameters and the type of failure mode witnessed for each specimen. Maximum values of σ_{max} and τ_{max} are computed according to Eqs. 2 and 3, respectively. It is highlighted that due to the early debonding observed for specimen DSL_SFRM_150_002, values of F_{max}, P_{max}, σ_{max} and τ_{max} for this specimen were disregarded for the calculation of the corresponding average.

$$\sigma_{max} = F/_{bt} \tag{2}$$

$$t_{max} = F/_{bl_b} \tag{3}$$

Table 2. Experimental results

SPECIMEN	F_{max} [kN]	P_{max} [kN]	σ_{max} [Mpa]	τ_{max} [Mpa]	Failure mode
DSL_SFRM_150_001	18.18	9.09	3.79	0.76	SFRM cracking
DSL_SFRM_150_002*	7.67	3.83	1.60	0.32	Early debonding
DSL_SFRM_150_003	19.92	9.96	4.15	0.83	Debonding + SFRM cracking
Average:	19.05	9.53	3.97	0.79	

*Disregarded

Results in Table 2 and Figure 4 show that the maximum value of F_{max} was obtained for specimen DSL_SFRM_150_003, followed by specimen DSL_SFRM_150_001 (around 10%

lower). Specimen DSL_SFRM_150_002 showed a significant lower value of F_{max} due to the occurrence of the early debonding of the SRM strip, as expressed above. Regarding σ_{max}, it is worth noting that values reported for specimens 001 and 003 are slightly lower than the tensile strength at first crack informed by the SFRM provider (see Table 1). These results indicate that the theoretical maximum value of F_{max} in the case of failure due to SFRM cracking might be related to the tensile strength at first crack of the material. However, further research in the topic is needed.

For the SFRM system and masonry substrate studied in this paper, results suggest that a bonded length (L_b) of 150 mm allows for the development of the maximum bond strength, whether failure is achieved by debonding or by SFRM cracking. As shown in Table 2, value of τ_{max} for specimen DSL_SFRM_150_003 was higher than that of specimen DSL_SFRM_150_001, although the former specimen failed by debonding and the latter by SFRM cracking. This result indicates that the SFRM strip tensile strength of specimen 001 might have been slightly lower than that of specimen 003. This difference allowed the failure of specimen DSL_SFRM_150_001 due to the SFRM cracking before the occurrence of the debonding. Therefore, for a SFRM strip with L_b=150mm and a higher value of tensile strength, failure will occur due to due to debonding from the substrate. On the other hand, on a SFRM strip with a low tensile strength, cracking and failure of the SFRM will occur before debonding.

4   CONCLUSIONS

The bond behavior of steel fiber reinforced mortar (SFRM) applied onto masonry substrates was investigated in this paper. With his aim, a series double-lap shear tests were performed on SFRM strips applied onto masonry wallets and the experimental results were discussed. Failure mode of the specimens was caused by debonding of the SFRM strip from substrate, with peeling-off of a thin layer of the masonry, SFRM cracking or a combination of both. For the SFRM bonded length studied in this paper (L_b=150mm), values of maximum applied load were similar whether failure was caused by debonding or SFRM cracking. This result suggests that the bonded length required to active the maximum bond strength in the SFRM material is close to 150 mm. Maximum values of axial stress in the SFRM strip were close to the tensile strength at first crack reported for the SFRM material. This indicates that, for the SFRM system and substrate studied in this paper, the maximum applied force, i.e., maximum bond strength, might be related to that parameter.

5   REFERENCES

ACI Committee 440 (2008) *Guide for the design and construction of externally bonded FRP systems for strengthening concrete structures*. ACI 440.2R. Farmington Hills, MI.

Altun, F., Haktanir, T. and Ari, K. (2007) 'Effects of steel fiber addition on mechanical properties of concrete and RC beams', *Construction and Building Materials*, 21(3), pp. 654–661. doi: 10.1016/j.conbuildmat.2005.12.006.

Askouni, P. D. and Papanicolaou, C. G. (2017) 'Experimental investigation of bond between glass textile reinforced mortar overlays and masonry: the effect of bond length', *Materials and Structures/Materiaux et Constructions*. Springer Netherlands, 50(2), pp. 1–15.

Bellini, A. and Mazzotti, C. (2017) 'A review on the bond behavior of FRP composites applied on masonry substrates', *RILEM Technical Letters*, 2, p. 74. doi: 10.21809/rilemtechlett.2017.40.

Carozzi, F. G., Poggi, C., Bertolesi, E. and Milani, G. (2018) 'Ancient masonry arches and vaults strengthened with TRM, SRG and FRP composites: Experimental evaluation', *Composite Structures*. Elsevier, 187(October 2017), pp. 466–480. doi: 10.1016/j.compstruct.2017.12.075.

Gonzalez-Libreros, J. H., Sneed, L. H., D'Antino, T. and Pellegrino, C. (2017) 'Behavior of RC beams

strengthened in shear with FRP and FRCM composites', *Engineering Structures*. Elsevier Ltd, 150, pp. 830–842.

Gonzalez-Libreros, J., Sabau, C., Sneed, L. H., Pellegrino, C. and Sas, G. (2017) 'State of Research on Shear Strengthening of RC Beams Using FRCM Composites', *Construction and Building Materials*. Elsevier Ltd, 149(September), pp. 444–458. doi: 10.1016/j.conbuildmat.2017.05.128.

Müller, S. and Mechtcherine, V. (2018) 'Use of Strain-Hardening Cement-Based Composites (SHCC) for Retrofitting', *MATEC Web of Conferences*, 199, p. 9006. doi: 10.1051/matecconf/201819909006.

National Research Council (CNR) (2013) *Guide for the design and construction of externally bonded FRP systems for strengthening existing structures*. CNR-DT 200. Rome, Italy.

Ombres, L., Mancuso, N., Mazzuca, S. and Verre, S. (2019) 'Bond between Carbon Fabric-Reinforced Cementitious Matrix and Masonry Substrate', 31(2009), pp. 1–11.

Sevil, T., Baran, M., Bilir, T. and Canbay, E. (2011) 'Use of steel fiber reinforced mortar for seismic strengthening', *Construction and Building Materials*, 25(2), pp. 892–899. doi: 10.1016/j.conbuildmat.2010.06.096.

Sneed, L. H., D'Antino, T., Carloni, C. and Pellegrino, C. (2015) 'A comparison of the bond behavior of PBO-FRCM composites determined by double-lap and single-lap shear tests', *Cement and Concrete Composites*. Elsevier Ltd, 64, pp. 37–48. doi: 10.1016/j.cemconcomp.2015.07.007.

De Stefano, M., Luciano, R., Focacci, F., Stipo, G., Alecci, V. and Rovero, L. (2017) 'Strengthening Masonry Arches with Lime-Based Mortar Composite', *Buildings*, 7(4), p. 49. doi: 10.3390/buildings7020049.

Tetta, Z. C. and Bournas, D. A. (2016) 'TRM vs FRP jacketing in shear strengthening of concrete members subjected to high temperatures', *Composites Part B: Engineering*. Elsevier Ltd, 106, pp. 190–205.

Tetta, Z. C., Koutas, L. N. and Bournas, D. A. (2015) 'Textile-reinforced mortar (TRM) versus fiber-reinforced polymers (FRP) in shear strengthening of concrete beams', *Composites Part B: Engineering*. Elsevier Ltd, 77, pp. 338–348.

Triantafillou, T. C. and Papanicolaou, C. G. (2006) 'Shear strengthening of reinforced concrete members with textile reinforced mortar (TRM) jackets', *Materials and Structures/Materiaux et Constructions*, 39(285), pp. 93–103.

Tsonos, A. D. G. (2014) 'A new method for earthquake strengthening of old R/C structures without the use of conventional reinforcement', *Structural Engineering and Mechanics*, 52(2), pp. 391–403. doi: 10.12989/sem.2014.52.2.391.

UNI 1015-11 (2007) 'Methods of test for mortar for masonry – Part 11: determination of flexural and compressive strength of hardened mortar'. Brussels, Belgium: EUROPEAN COMMITTEE FOR STANDARDIZATION.

UNI EN 13412 (2006) 'Products and systems for the protection and repair of concrete structures. Test methods. Determination of modulus of elasticity in compression'. Brussels, Belgium: EUROPEAN COMMITTEE FOR STANDARDIZATION.

Vaculik, J., Visintin, P., Burton, N. G., Griffith, M. C. and Seracino, R. (2018) 'State-of-the-art review and future research directions for FRP-to-masonry bond research: Test methods and techniques for extraction of bond-slip behaviour', *Construction and Building Materials*. Elsevier Ltd, 183, pp. 325–345. doi: 10.1016/j.conbuildmat.2018.06.103.